Energy Conversion and Management 132 (2017) 347–360

Contents lists available at ScienceDirect

Energy Conversion and Management

journal homepage: www.elsevier.com/locate/enconman

Analysis of the backpressure effect of an Organic Rankine Cycle (ORC) evaporator on the exhaust line of a turbocharged heavy duty diesel power generator for marine applications

Constantine N. Michos [a], Simone Lion [a,b,*], Ioannis Vlaskos [a], Rodolfo Taccani [b]

[a] Ricardo Deutschland GmbH, Schwäbisch Gmünd, Germany
[b] University of Trieste, Trieste, Italy

ARTICLE INFO

Article history:
Received 8 August 2016
Received in revised form 11 November 2016
Accepted 12 November 2016

Keywords:
Marine engine
Organic Rankine Cycle
Turbocharging
Engine backpressure
Optimization

ABSTRACT

In marine and power generation sectors, waste heat recovery technologies are attracting growing attention in order to increase heavy duty diesel engines efficiency and decrease fuel consumption, with the purpose of respecting stringent emissions legislations.

In this work, the backpressure effect of an Organic Rankine Cycle (ORC) evaporator on the exhaust line of a turbocharged, V12 heavy duty diesel engine, for typical marine and power generation applications has been investigated using the commercial software Ricardo WAVE. Three different state-of-the art turbocharging strategies are assessed in order to counterbalance the increased pumping losses of the engine due to the boiler installation: fixed turbine, Waste-Gate (WG) and Variable Geometry Turbine (VGT). At the same time, the steady-state thermodynamic performance of two different ORC configurations, simple tail-pipe evaporator and recuperated simple tail-pipe evaporator layouts, are assessed, with the scope of further increasing the engine power output, recovering unutilized exhaust gas heat. Several different working fluids, suitable for medium-high temperature waste heat recovery, are evaluated and screened, considering, as well, health and safety issues. Thermodynamic cycle parameters such as, for example, evaporation and condensing pressures, working fluid mass flow and cycle temperatures, are optimized in order to obtain the maximum improvement in Brake Specific Fuel Consumption (bsfc).

From the engine side point of view, a VGT turbocharger is the most favorable solution to withstand increased backpressure, while, regarding the ORC side, between the considered fluids and layouts, acetone and a recuperated cycle show the most promising performance.

1. Introduction

Organic Rankine Cycle (ORC) technologies for large marine diesel engines are constantly gaining increased interest as waste heat recovery solutions by engine and ORC system manufacturers due to their potential of considerably decreasing fuel consumption, operating costs and greenhouse gas emissions, as can be evidenced by relevant commercial activities in the market [1–3].

Systems proposed in feasibility studies, or already fully integrated on board ships, are meant to recover heat from a number of different sources, such as, for example, exhaust gas, jacket cooling water, lube oil and charge air, using cycle configurations of various levels of complexity and organic working fluids usually selected according to the temperature level of the heat source, in order to maximize thermodynamics performance.

Furthermore, ORC systems are also under development to recover heat from lower temperature heat sources from two stroke marine propulsion unit of MW size, in particular, focusing on engine jacket water heat recovery [4].

However, fitting an Organic Rankine Cycle (ORC) system on the exhaust line of an engine has also some drawbacks: for example, safety issues, due to possible fluid-exhaust gas contact, increased weight and complexity of the overall system and increased engine backpressure, which could lead to performance degradation. As discussed in this paper, engine backpressure can be counterbalanced implementing appropriate turbocharging strategies.

The literature about engine backpressure and turbocharging strategies in marine applications is rather sparse [5–9]. In [5–7] the development of a control strategy to improve engine performance by dynamically varying the turbine nozzle area in response

* Corresponding author at: Ricardo Deutschland GmbH, Güglingstraße 66, Schwäbisch Gmünd 73529, Germany.
E-mail addresses: simone.lion@ricardo.com, simone.lion@phd.units.it (S. Lion).

http://dx.doi.org/10.1016/j.enconman.2016.11.025
0196-8904/

Nomenclature

bmep	brake mean effective pressure, bar
bsfc	brake specific fuel consumption, g kWh^{-1}
c_p	specific heat, kJ kg^{-1} °C^{-1}
$\dot{m}_f$	mass flow, kg s^{-1}
N	engine speed, rpm
n_{cyl}	number of cylinders
p	pressure, bar
PMEP	pumping mean effective pressure, bar
q	amount of specific heat exchanged, kJ kg^{-1}
$\dot{Q}$	heat transfer rate, kW
SI	Surface Index, kJ kg^{-1} °C^{-1}
T	temperature, °C
UA	heat transfer coefficient, W °C^{-1}
v	specific volume, m^3 kg^{-1}
V_d	engine displacement, l
w	specific work, kJ kg^{-1}
$\dot{W}$	power, kW
Δp	pressure drop, mbar
ΔT	temperature drop, °C

Greek symbols

ε	effectiveness
η	efficiency
ρ	density, kg m^{-3}

Subscripts

boil	boiling (temperature)
brake	brake (power)
cond	condensation
c	critical point
cw	cooling water
cyl	cylinder
e	electrical
E	expander
EG	exhaust gas
eng	engine
evap	evaporation
freeze	freezing (temperature)
fuel	fuel (injected)
HL	heat losses
in	inlet
is	isentropic
liq	liquid
m	mechanical
max	maximum (temperature)
net	net
out	outlet
P	pump
pp	pinch point
ratio	ratio (evaporation/condensation pressure)
rec	recovery
subc	sub-cooling
suph	super-heating
TC	turbocharger
th	thermal (efficiency)
TO	thermal oil (carrier fluid)
wf	working fluid
vap	vapour

Acronyms

AFR	Air Fuel Ratio
C	Compressor
CAC	Charge Air Cooler
CFC	Chlorofluorocarbon
CNDR	Condenser
CWHX	Cooling Water Heat Exchanger
DSUP	Desuperheater
E	Expander
EES	Engineering Equation Solver
EGHX	Exhaust Gas Heat Exchanger
EVAP	Evaporator
GWP	Global Warming Potential
HCFC	Hydrochlorofluorocarbon
HFC	Hydrofluorocarbon
HX	Heat Exchanger
IMO	International Maritime Organization
LMTD	Log Mean Temperature Difference
LNG	Liquefied Natural Gas
MFR	Mass Flows Ratio
NFPA	National Fire Protection Agency
NOx	Nitrogen oxides
ODP	Ozone Depletion Potential
ORC	Organic Rankine Cycle
PRHT	Preheater
RECP	Recuperator
RORC	Regenerative Organic Rankine Cycle
SCR	Selective Catalytic Reduction
SOI	Start Of Injection
SUBC	Subcooler
SUPH	Superheater
T	Turbine
TOHX	Thermal Oil Heat Exchanger
VER	Volumetric Expansion Ratio
VGT	Variable Geometry Turbine
WG	Waste-Gate
WHR	Waste Heat Recovery

to backpressure variations is presented. A novel supercharged-turbocharged system was also proposed by Hermann [8] in order to deal with steady-state and dynamic backpressure conditions for submarine engines, while Hield [9] presented the detailed results of the response of a turbocharged diesel engine to steady-state and dynamic backpressure variations, with emphasis focused on interpreting the relevant processes.

The topic is often discussed in literature for applications other than marine, such as vehicles and few hundreds kW size stationary engines.

For example, Katsanos et al. [10] presented a theoretical study to investigate the waste heat recovery efficiency potential of a Rankine cycle applied to a heavy duty truck diesel engine. A maximum fuel economy of about 10.2% is obtained from simulations results, and engine backpressure is also discussed.

Horst et al. [11] proposed a dynamic simulation model, validated with test bench measurements, to predict fuel saving potential over a dynamic motorway scenario. The authors observed that a waste heat recovery system, as an ORC, can improve fuel efficiency of about 3.4%, but effects such as weight increase and increased engine backpressure are not negligible. An average between 20 and 5 mbar backpressure can be expected for a steady state high speed driving condition but higher backpressure can be reached during acceleration peaks.

Bei et al. [12] proposed a simulation model of an ORC fin-and-tube evaporator using a CFD approach. The engine side is modelled using a 1-D approach. A limited backpressure (up to 2 mbar) is reported for the four cylinders turbocharged engine considered, with an estimated fuel consumption increase of 1%.

Di Battista et al. [13] discussed the effects of the backpressure increase due to the installation of an ORC plate heat exchanger on the tail-pipe of a turbocharged IVECO F1C 3.0 L engine for light-duty commercial vehicles propulsion. The proposed plate boiler leads to a high backpressure increase of more than 250 mbar. They concluded that a VGT turbine strategy can mitigate the increased pumping losses drawback effect. Boiler off-design operating conditions and weight increase problems are also investigated.

Allouache et al. [14] reported a study about fitting an exhaust heat exchanger on the tailpipe of a 6.7 L Cummins heavy duty diesel engine. The heat exchanger has been tested in order to optimize the pressure drop using R245fa as ORC working fluid. An estimation of the recovery potential and engine thermal efficiency improvement, in the range of 5% over the entire load/speed range, is also reported.

Yamaguchi et al. [15] presented a feasibility study about the recovery of exhaust gas heat from a 6 cylinders heavy duty diesel engine with high pressure and low pressure EGR (Exhaust Gas Recirculation) circuits, as well as two different boosting strategies to counterbalance the increased backpressure. An improvement in fuel economy of 2.7% with single-stage and 2.9% with double-stage turbocharging architecture, on highway cruising conditions at 80 km/h constant speed, has been reported when using an ORC system.

In literature, several studies are available about the introduction of ORC in marine applications, but not all of them consider also the effect on the internal combustion engine.

Song et al. [16] studied the waste heat recovery potential of an ORC to recover heat from the cooling water and the exhaust gas of a medium speed 996 kW marine diesel engine produced by Hudong Machinery Co., Ltd. Economic evaluations as well as off-design conditions are considered. An optimized system using cyclopentane, cooling water as preheating source and exhaust gas as evaporating source for the working medium is proposed, obtaining only around 1.4% lower power output compared to the separated bulkier systems.

Reini et al. [17] proposed a study about recovering waste heat from the exhaust gas of marine dual-fuel engine with power output of 5.7 MW. The selected working fluid is toluene and a simple cycle architecture has been considered the most interesting in terms of increased power output benefits. A thermo-economic analysis, considering the payback period, has also been carried out.

Burel et al. in [18] analysed the possibility to install and ORC in a tanker where Liquefied Natural Gas (LNG) is used as propulsion fuel.

Baldi et al., in two different works [19,20], proposed the use of optimization techniques for diesel engine-ORC waste heat recovery systems based on the analysis of typical ships operating profiles. The case studies use, as baseline engines, MaK 8M32C four-stroke diesel engines with a power output of 3840 kW and some auxiliary units of about 683 kW. Fuel saving potential is considered for some typical vessels applications.

Yun et al. [21] proposed a study about a dual loop ORC system with the aim of recovering waste heat in parallel from the exhaust gas of marine diesel engines, with the highlighted benefit of being more versatile when operating at off design conditions. The conclusion is that the dual loop ORC has a power output which is between 3 and 15% higher than a simple single system.

Yfantis et al. [22] proposed a thermodynamic model to study the first and second law performance characteristics of a four stroke marine diesel engine equipped with a Regenerative Organic Rankine Cycle (RORC) to recover exhaust heat. Different engine operating loads are investigated, as well as R245fa, R245ca, isobutane and R123 as working fluids. A subcritical and saturated vapour regenerative cycle is found to have the best performance both from first and second law point of view.

Two-stroke ship propulsion units are also considered, for example in [23–26], usually with the hypothesis of recovering heat from exhaust gas, cooling jacket water and scavenge air.

In this work, the interactions between a modern marine turbocharged diesel power generation unit and a possible exhaust gas driven ORC system, for combined system efficiency improvement, are investigated through simulation.

In particular, both internal combustion engine and ORC sides are investigated, considering different engine turbocharging strategies and the optimization of the ORC cycle parameters in order to obtain the best combined fuel consumption reduction.

On the engine side, the adverse backpressure effect of fitting an exhaust gas driven ORC evaporator on the engine breathing capabilities, is investigated using Ricardo plc proprietary 1-D engine performance simulation software Ricardo WAVE [27]. Fixed geometry, Waste-Gate (WG) and Variable Geometry Turbocharger (VGT) boosting technologies are evaluated in order to withstand the increased pumping losses due to the waste heat recovery boiler installation.

On the ORC side, for each of the three investigated turbocharging system scenarios and for a moderate exhaust gas backpressure, which corresponds to specific exhaust gas characteristics (mass flow rate and temperature), the power output of optimized, in terms of thermodynamic cycle parameters, simple and recuperated exhaust gas driven ORC layouts is computed using Engineering Equation Solver (EES, [28]) for a set of working fluids (*n*-hexane, *n*-octane, acetone, toluene, ethanol and MDM) selected after a screening procedure, which considers not only thermodynamic performance, but also environmental, flammability and safety issues. After identifying the most promising turbocharging system-ORC configuration, in terms of combined system fuel economy improvement for the moderate backpressure case, further simulations of this system have been performed for a range of backpressure values in order to evaluate the corresponding expected range of fuel economy benefit for all possible heat exchangers hardware designs.

2. Baseline engine model

The simulation model has been implemented using Ricardo WAVE [27], considering a 1.5 MW high speed diesel engine (120 kW/Cylinder at 1500 rpm) running at full load conditions.

The engine configuration is a V12, with single-stage turbocharging and aftercooler, employing Miller inlet valve timing for reduced NO_x emissions. The engine is used in the power generation or marine sector as a generator set and equipped with a Selective Catalytic Reduction (SCR) system for compliance with IMO (Internal Maritime Organization) Tier III NO_x emissions regulations [29]. Some of the basic geometric features and full load performance data of the engine at ISO ambient conditions (25 °C, 1 bar) are reported in Table 1.

It is assumed that, at the above reported ambient conditions, the pressure drops of the SCR system and the Charge Air Cooler (CAC) are respectively 120 mbar and 100 mbar, while the outlet temperature of the CAC and the efficiency of the SCR system are always constant, being respectively 55 °C and 65%. It has to be noted that the SCR efficiency determines the maximum allowable engine NO_x emissions, which are in turn controlled in the engine WAVE model by regulating the injection timing. This parameter

Table 1
Basic engine features and full load performance data at ISO ambient conditions (baseline engine case).

Displacement/cylinder (l)	V_d	4.31
No of cylinders	n_{cyl}	12
Speed (rpm)	N	1500
Brake mean effective pressure (bar)	$bmep$	22
AFR trapped (–)	AFR	27
IMO Tier III NOx limit (g/kWh)	–	2.0
Baseline turbocharging efficiency (%)	η_{TC}	59.0

is also controlled in order to avoid to have peak cylinder pressures in excess of 230 bar.

Another constraint, related to safe turbocharger turbine steady-state operations, is that the inlet temperatures should not be higher than 700 °C.

The model simulates the combustion process in a simplified way, using an experimentally derived, non-dimensional burn rate profile, which is valid under the examined engine speed, trapped Air-Fuel-Ratio (AFR) and typical start of injection (SOI) timings. To simplify the calculations, it is assumed that the turbocharger efficiency remains constant. The turbine and compressor are modelled with a quasi-steady approach, calculating the mass flow and enthalpy rise across the components, simulated as an orifice, as well as the torque produced or absorbed.

Considering that the SCR thermochemical performance is not modelled and considered in this work, it is assumed that, under steady-state operating conditions, the exhaust gas temperature downstream the turbocharger turbine is equal to the inlet temperature of the Exhaust Gas Heat Exchanger (EGHX or boiler) of the ORC system (no temperature change is assumed over the SCR system, following what reported by Qiu et al. [30]).

The ORC boiler is installed downstream the SCR system, as reported in Fig. 1, which describes the layout of the combined Engine-EGHX. The location of the boiler is selected so that the SCR performance is practically unaffected.

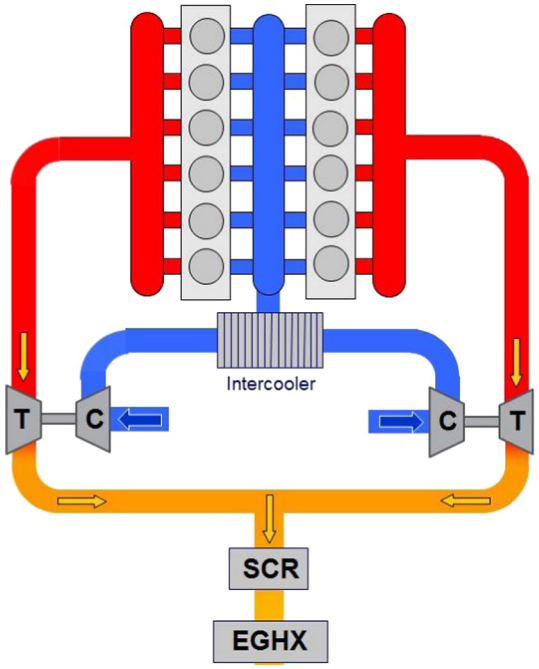

Fig. 1. Combined engine-ORC EGHX layout scheme.

2.1. Turbocharging systems description

In a common turbocharger design for large four-stroke engines, an exhaust gas driven radial or axial turbine is coupled to a centrifugal air compressor. The engine exhausted gas drives the turbine which is coupled to the compressor in order to increase the intake boost pressure, thus also increasing engine volumetric efficiency and performance [31].

Three turbocharging systems are analysed: (1) fixed geometry turbine, (2) Waste-Gate (WG) and (3) Variable Geometry Turbocharging (VGT).

The simplest turbocharger configuration is with fixed geometry for both compressor and turbine. In this case, there is no boost control possibility, and the boost level is directly related to the exhaust gas flow and to the turbocharger characteristics. The enthalpy to drive the turbine is directly dependent on the combustion performance.

The WG turbocharging strategy uses a waste gate valve to bypass the turbine in order to control the rotational speed of the turbocharger, thus regulating the boost pressure of the engine. Adding a by-pass valve to the fixed geometry turbocharger is the easiest implementable strategy to improve engine control over a more severe transient operational profile or over more variable backpressure conditions. However, typically, WG turbochargers increase the exhaust losses, thus leading to decreased turbocharger efficiency [32].

The VGT operates altering the geometry of the effective turbine area in order to reach the requested boost pressure for the compressor, but still handling all the exhaust flow, which does not bypass the turbine. This turbocharging strategy usually allows better control of boost pressures at low engine loads and speeds. In particular, for large medium-low speed diesel engines, the VGT are equipped with a nozzle ring with movable vanes which direct the exhaust gas flow through the turbine blades. The angle of the vanes is controlled at different engine speeds in order to optimize the flow through the turbine [33]. A precise control of AFR can be obtained with this strategy, as well as losses associated with the Waste-Gate valve are eliminated and engine control improved [31]. Drawbacks of VGT are the increased cost and vanes fouling problems when using heavy fuel oils [32].

In this preliminary study, a parametric analysis of the ORC boiler backpressure effect has been carried out considering the three turbocharging solutions and assuming the engine operating at full load constant conditions.

The backpressure range considered is from 0 to 100 mbar in order to study different boiler designs.

When considering the Waste-Gate solution (Case 2), the turbocharger is dimensioned, at the highest backpressure case (100 mbar), with fully closed waste gate valve, thus resulting in a smaller turbine than that used in Case 1 with fixed geometry turbocharger. The dimensioning aims also to maintain the AFR at the design point value. Then, as the backpressure is reduced, the waste gate valve is gradually opened in order to keep the requested AFR always constant.

In the Case 3, the turbine nozzle area of the VGT turbocharger is controlled in order to keep, again, the AFR constant, independently of the EGHX backpressure imposed.

3. Organic Rankine Cycle (ORC) modelling

In the following paragraphs an overview of the considered cycle architectures, of the proposed modelling and optimization approach and working fluid selection procedure is presented with reference to the ORC system section.

3.1. Cycle architectures and modelling approach

In terms of ORC system layouts, a simple and a recuperated cycle are examined, both employing an intermediate thermal oil circuit [34].

The cooling medium in the condenser is water, which could hypothetically be sea water, and easily available on-board ships.

The schemes of the two cycle architectures considered are reported in Fig. 2.

For modelling reasons, the Thermal Oil Heat Exchanger (TOHX) and the Cooling Water Heat Exchanger (CWHE) are divided respectively in three regions, in which preheating (PRHT), evaporation (EVAP), superheating (SUPH), de-superheating (DSUP), condensing (CNDR) and sub-cooling (SUBC) processes happen.

For every region, a fixed boundary modelling technique is applied, as well as mass and energy balances.

In the case of the Exhaust Gas Heat Exchanger (EGHX), a unique region is considered, since no phase change is happening. The same approach is used for the recuperator (RECP).

All the heat exchangers are considered to have a counter-flow configuration in order to increase heat transfer efficiency.

The pump and expander (E) are modelled with a simple fixed isentropic efficiency, considered for steady-state full load operations.

Two examples of T-s diagrams are reported in Fig. 3 in the case of *n*-hexane working fluid, for the simple and recuperated cycles.

In the case of the recuperated cycle, a recuperator (RECP) is added in order to partially preheat the liquid working fluid downstream the pump using the heat rejected from the superheated vapour at the expander outlet. The purpose of this second configuration is to increase the ORC system efficiency thus leading to a better utilization of the engine recovered heat.

For the ORC modelling, first of all, the condensing pressure is fixed to the minimum possible, considering heat sink and ambient constraints. In this case, the condensing pressure is fixed to 1 bar to avoid possible air infiltration in the system.

The working fluid is pressurized by the pump from the condensation pressure to the evaporation pressure, thus fixing the pressure levels of the system:

$$p_{evap} = p_{ratio} \cdot p_{cond} \tag{1}$$

The isentropic pumping specific work is calculated, assuming constant specific volume, from the following formula:

$$w_{P,is} = v_{P,in} \cdot (p_{P,in} - p_{P,out}) \tag{2}$$

A fixed isentropic efficiency approach has been used to calculate the pumping required specific work:

$$w_P = \frac{w_{P,is}}{\eta_P} \tag{3}$$

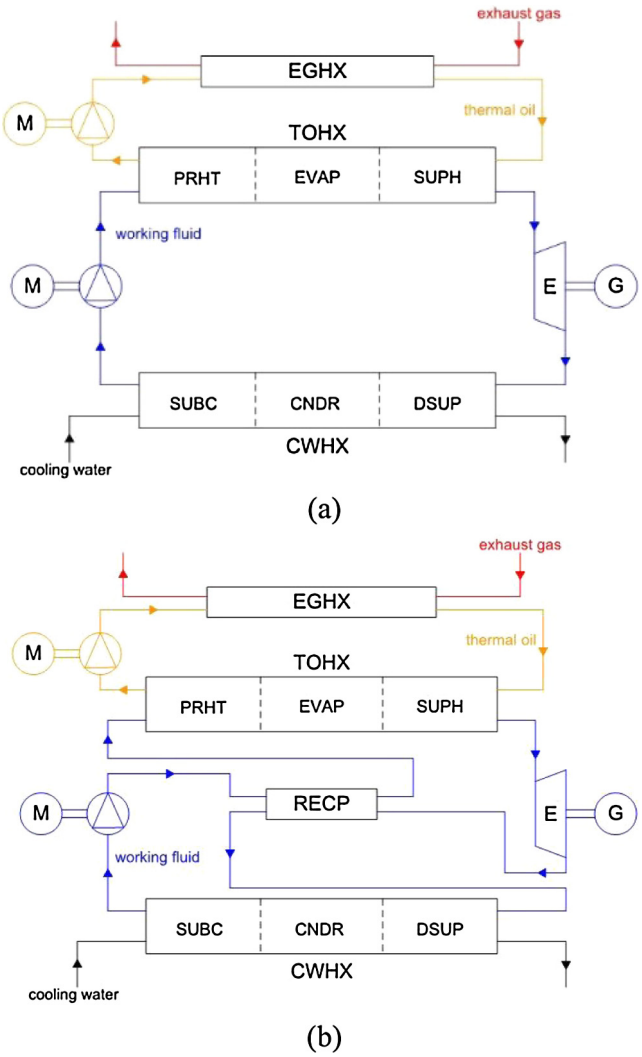

Fig. 2. Schemes of the simple (a) and recuperated (b) ORC layouts.

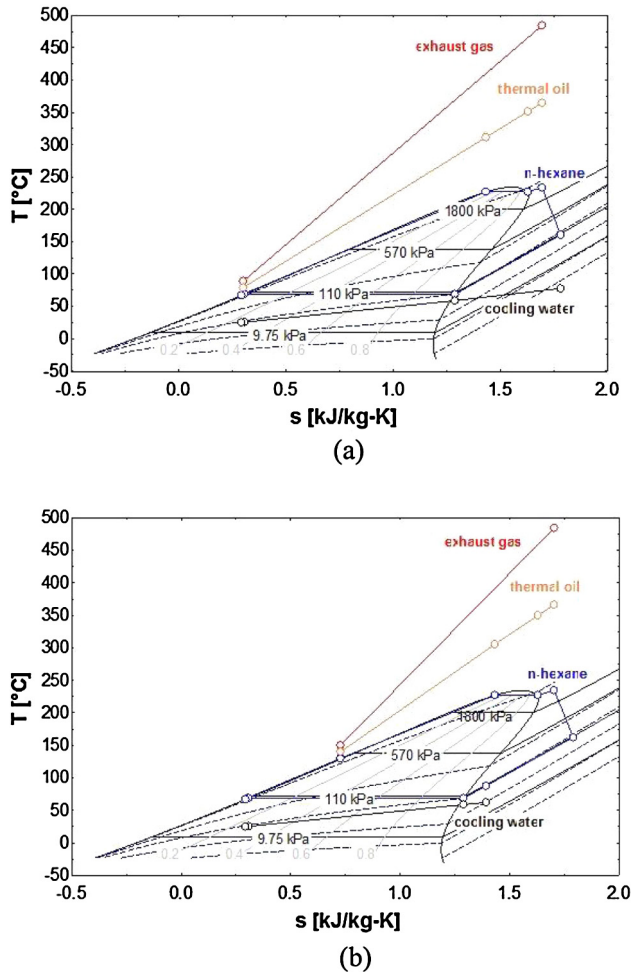

Fig. 3. *n*-hexane T-s diagram examples for simple (a) and recuperated (b) ORC.

The properties of the thermal oil and, in particular, the specific heat, have been obtained from [34], and a correlation has been calculated based on the temperatures at the inlet and outlet of the heat exchangers and pump of the oil circuit:

$$c_{p,TO} = 0.003 \cdot T_{TO} + 1.6017 \tag{4}$$

An average specific heat value has been used, between inlet and outlet of the heat exchangers components, in order to calculate the heat balances (the exhaust gas specific heat has been considered constant).

For the exhaust gas heat exchanger (EGHX) the balance considers only one zone, since no thermal oil evaporation is expected:

$$\dot{m}_{f,TO} \cdot c_{p,TO} \cdot (T_{TO,EGHX,out} - T_{TO,EGHX,in}) = \dot{m}_{f,EG} \cdot c_{p,EG} \cdot (T_{EG,EGHX,in} - T_{EG,EGHX,out}) \tag{5}$$

For the thermal oil heat exchanger (TOHX), in contact with the ORC working fluid, the process has been divided between preheating (PRHT), evaporation (EVAP) and superheating (SUPH). Heat balance equations have been applied for the considered three zones, using average specific heat values for the working fluid and thermal oil sides:

$$\dot{m}_{f,wf} \cdot q_{PRHT} = \dot{m}_{f,TO} \cdot c_{p,TO} \cdot (T_{TO,PRHT,in} - T_{TO,PRHT,out}) \tag{6}$$

$$\dot{m}_{f,wf} \cdot q_{EVAP} = \dot{m}_{f,TO} \cdot c_{p,TO} \cdot (T_{TO,EVAP,in} - T_{TO,EVAP,out}) \tag{7}$$

$$\dot{m}_{f,wf} \cdot q_{SUPH} = \dot{m}_{f,TO} \cdot c_{p,TO} \cdot (T_{TO,SUPH,in} - T_{TO,SUPH,out}) \tag{8}$$

The same approach has been used in order to calculate the heat balances for the three zones in which the condenser has been divided: de-superheating (DSUP), condensation (CNDR) and sub-cooling (SUBC). For the cooling water, the specific heat has also been considered constant for an average temperature level. The heat balances for the condensing side can be written as follows:

$$\dot{m}_{f,wf} \cdot q_{DSUP} = \dot{m}_{f,cw} \cdot c_{p,cw} \cdot (T_{cw,DSUP,out} - T_{cw,DSUP,in}) \tag{9}$$

$$\dot{m}_{f,wf} \cdot q_{CNDR} = \dot{m}_{f,cw} \cdot c_{p,cw} \cdot (T_{cw,CNDR,out} - T_{cw,CNDR,in}) \tag{10}$$

$$\dot{m}_{f,wf} \cdot q_{SUBC} = \dot{m}_{f,cw} \cdot c_{p,cw} \cdot (T_{cw,SUBC,out} - T_{cw,SUBC,in}) \tag{11}$$

In the case of the recuperated ORC system (RECP), the heat exchanged between the liquid and vapour sides of the heat exchanger is calculated from an iterative procedure solved in EES, in order to obtain the vapour side outlet temperature $T_{vap,RECP,out}$ and the liquid side outlet temperature $T_{liq,RECP,out}$. The considered specific heat is the minimum between the average values calculated at the liquid and vapour sides, and it is dependent on the outlet temperatures. The balance over the recuperator has been calculated with the following formula, assuming a fixed heat exchange effectiveness, ε_{RECP}, of 80%:

$$q_{RECP} = \varepsilon_{RECP} \cdot c_{p,min} \cdot (T_{vap,RECP,in} - T_{liq,RECP,out}) \tag{12}$$

The thermal oil circuit pump power consumption has been estimated based on an assumed averaged 80 mbar pressure drop over both the two heat exchangers, from the following formula:

$$\dot{W}_{P,TO,is} = \frac{(\Delta p_{TO,TOHX} + \Delta p_{TO,EGHX}) \cdot \dot{m}_{f,TO}}{\rho_{TO} \cdot \eta_{P,TO}} \tag{13}$$

The pump fixed isentropic efficiency ($\eta_{p,TO}$) is 60%.

The thermal oil density has been calculated, as previously done for the specific heat, with the following formula, fitted from the curve reported in [34]:

$$\rho_{TO} = -0.7543 \cdot T_{TO} + 979.25 \tag{14}$$

The expander specific work (w_E) has been calculated assuming a fixed isentropic efficiency (η_E) of 70%, with the following formula, where $w_{E,is}$ is the isentropic enthalpy:

$$w_E = w_{E,is} \cdot \eta_E \tag{15}$$

Finally, the ORC net specific work has been obtained as:

$$w_{ORC,net} = w_E - w_P \tag{16}$$

Net ORC power ($\dot{W}_{ORC,net}$), expander produced power ($\dot{W}_E$) and pump required power ($\dot{W}_P$) have then been calculated multiplying the specific work values for the working fluid mass flow rate.

The ORC cycle thermal efficiency has been calculated considering the thermal oil heat exchanger (TOHX) heat input, q_{in}, and the cycle net specific work:

$$\eta_{ORC,th} = \frac{w_{ORC,net}}{q_{in}} \tag{17}$$

The combined system brake specific fuel consumption (bsfc), when using the ORC on the engine exhaust line, is calculated with the following formula:

$$bsfc_{eng+ORC} = \frac{\dot{m}_{f,fuel}}{(\dot{W}_{brake} + \dot{W}_{ORC,net})} \tag{18}$$

3.2. Working fluid selection

In order to limit the number of working fluids to be investigated through simulation, a selection procedure is conceived and applied, based on environmental (legislative), safety, usage and thermodynamic requirements.

According to control measures dictated by the Montreal protocol [35] on substances which deplete the ozone layer, the use of chlorofluorocarbons (CFCs), such as for example R11, R12, R13, R113, R114 and R115, has been already totally banned since 2010, while the use of Hydro-Chloro-Fluorocarbons (HCFCs), such as for example R21, R22, R123, R124, R141b and R142b, will be practically banned from 2020, due to the high ozone depletion potential of these substances due mainly to their chlorine content.

At the same time, the Kyoto protocol [36] on greenhouse gas emissions defined the percentage emissions reduction commitment of various countries, including Hydro-Fluoro-Carbons (HFCs), e.g. R23, R32, R125, R134a, R143a, R152a, R236ea, R236fa, R245ca, R245fa and R365mfc, among the listed (but not banned) gases due to their high global warming potential (GWP).

Based on these environmental limitations, various working fluids (pure substances and mixtures) from the relevant literature as well as from real applications for low- [37] and high-temperature [38] ORC applications are considered at the starting point of the selection procedure and categorised into families, as shown in Table 2.

Due to safety issues, the environment in which the ORC system is going to operate should always be taken into consideration. For this reason, the generally applicable NFPA 704 Standard is used in this work to characterise the severity level of each working fluid in terms of health, flammability, and instability hazards, based on the values shown in Table 3 [39]. As a rule, working fluids with 'Health Hazard' higher than 2 and 'Flammability Hazard' higher than 3 are excluded and not considered in the simulation work.

In terms of usage requirements, working fluids with freezing temperatures higher than approximately −30 °C should be also excluded, in order to avoid freezing problems during very cold days, unless the ORC is installed in a temperature controlled environment.

Specific thermodynamic requirements must also be considered in the simulations.

Table 2
Working fluids considered at the starting point of the selection procedure.

Linear and branched hydro-carbons	Aromatic hydro-carbons	HFCs[a]	Fluoro-Carbons	Inorganic fluids	Alcohols	Siloxanes	Zeotropic mixtures
i-butane	Cyclopropane	R134a	C5F12	Water	Ethanol	MDM	Ammonia/water 20/80
Pentane	Benzene	R236fa	RC318	Ammonia		MM	R32[a]/R134a[a]30/70
n-hexane	Toluene	R245fa					R125[a]/R245fa[a] 90/10
n-octane	*p*-xylene	R365mfc					R245fa[a]/R152a[a] 45/55
Acetone							R245fa[a]/pentane 50/50

[a] Listed in the Kyoto protocol.

Table 3
NFPA 704 standard for health, flammability, instability hazards.

Health hazard	Flammability hazard	Instability hazard
4 – Can be lethal	**4** – Will vapourize and readily burn at normal temperatures	**4** – May explode at normal temperatures and pressures
3 – Can cause serious or permanent injury	**3** – Can be ignited under almost all ambient temperatures	**3** – May explode at high temperature or shock
2 – Can cause temporary incapacitation of residual injury	**2** – Must be heated or high ambient temperature to burn	**2** – Violent chemical change at high temperatures or pressures
1 – Can cause significant irritation	**1** – Must be preheated before ignition can occur	**1** – Normally stable. High temperatures make unstable
0 – No hazard	**0** – Will not burn	**0** – Stable

At the low pressure side of the ORC system, the condensation pressure should be higher than the ambient pressure in order to avoid air infiltration into the system, while the condensation temperature should be higher than approximately 50 °C, to prevent reverse heat transfer from ambient to the working fluid during very hot days. These constraints are graphically reported in Fig. 4, where the saturation curves of most of the considered fluids of Table 2 are presented.

As shown, the upper right (white) window represents the practical condensation region of the various fluids. In particular, regarding HFCs and fluorocarbons, it can be observed that the condensation pressure must be relatively high, resulting consequently in reduced available expansion ratios for the ORC expander and consequently lower power production.

With similar considerations, at the high pressure side, the evaporation pressure should be lower than the critical pressure of the working medium, in order to avoid fluid degradation effect, as well as a limit of 30 bar for the maximum cycle pressure has been set to avoid material strength issues. Moreover, the evaporation temperature should be higher than 50 °C to again prevent reverse heat transfer during operations in very hot environments or climate conditions.

As an appropriate guideline, fluids whose critical temperature is higher than 200 °C should be considered suitable for medium-high temperature ORC applications such as the one in the considered case study.

All previously described requirements and constraints, applied separately to each of the various fluids of Table 2, are collectively presented in Table 4. Each fluid is evaluated against the requirements successively and, when not passing one of them, it will be discarded and not analysed in the following simulation work. From the original set of candidate fluids, it can be seen that only six of them are appropriate for the developed case study, considering the described constraints. The appropriate fluids are reported in bold letters in Table 4 and in Table 5 with the respective main properties, obtained from NIST REFPROP [40].

3.3. Basic assumptions and constraints for ORC system optimization

The basic assumptions and constraints for the ORC investigated in this work are presented in Table 6. The cycle independent variables for the optimization procedure are reported in Table 7. A Genetic Algorithm has been applied, with the purpose of maximizing the ORC net power output. The ORC engine exhaust gas boundary conditions are reported, for every turbocharging case evaluated, in Fig. 5(k)–(l).

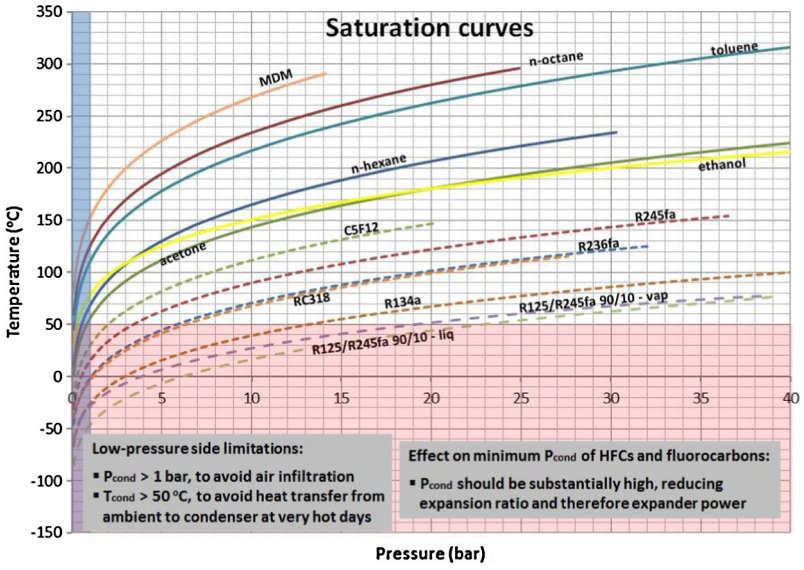

Fig. 4. ORC system low pressure side limitations on working fluids saturation curve diagram.

Table 4
Working fluid selection procedure. In bold the selected fluids for the simulations runs. In italics the design requirements.

Working fluid	Health hazard (–)	Flammability hazard (–)	Freezing temperature T_{freeze} (°C)	Condensation pressure p_{cond} (bar)	Evaporation pressure p_{evap} (bar)	Critical temperature T_c (°C)
Requirement	*⩽2*	*⩽3*	*<−30 °C*	*Available range should be significant*		*>200 °C for high temp. applications*
i-butane	1	4	–	–	–	–
Pentane	1	4	–	–	–	–
***n*-hexane**	**2**	**3**	**−95.3**	**>1**	**<30**	**234.7**
***n*-octane**	**1**	**3**	**−56.6**	**>1**	**<25**	**295.2**
Acetone	**1**	**3**	**−94.7**	**>1**	**<30**	**235**
Cyclopentane	1	4	–	–	–	–
Benzene	2	3	5.5	–	–	–
Toluene	**2**	**3**	**−95.2**	**>1**	**<30**	**318.6**
p-xylene	2	3	13.3	–	–	–
R134a	1	0	−103.3	>13.2	<30	101.1
R236fa	1	0	−93.6	>5.9	<30	124.9
R245fa	2	0	−102.1	>3.5	<30	154
R365mfc	0	4	–	–	–	–
C5F12	1	1	−120	>2.1	<20.5	147.4
RC318	2	0	−40	>6.5	<27.8	115
Water	0	0	0	–	–	–
Ammonia	3	–	–	–	–	–
Ethanol	**2**	**3**	**−114.2**	**>1**	**<30**	**241.6**
MDM	**0**	**3**	**−86**	**>1**	**<14.2**	**290.9**
MM	1	4	–	–	–	–
Ammonia/water 20/80	3/0	–	–	–	–	–
R32/R134a 30/70	1/1	4/0	–	–	–	–
R125/R245fa 90/10	1/2	0/0	−107	>22.9	<30	–
R245fa/R152a 45/55	2/1	0/4	–	–	–	–
R245fa/pentane 50/50	2/1	0/4	–	–	–	–

Table 5
Working fluids evaluated for the simulation work.

Working fluid	T_c (°C)	p_c(bar)	T_{boil} (°C)	T_{freeze} (°C)
n-hexane	234.7	30.4	68.7	−95.3
n-octane	295.2	25	125.6	−56.6
Acetone	235	47	56.1	−94.7
Toluene	318.6	41.3	110.6	−95.2
Ethanol	241.6	62.7	78.4	−114.2
MDM	290.9	14.2	152.5	−86

Regarding the condenser, a slight sub-cooling is usually applied to ensure that the working fluid, at the inlet of the pump, is in a liquid state, even if the fluid receiver is not modelled in this study for simplicity reasons.

Regarding the exhaust gas temperature downstream the EGHX, it should be usually higher than the acid dew point temperature of the gas, in order to ensure that no condensation of corrosive sulphuric acid occur on the last section of the heat exchanger. For IMO Tier III complying marine Diesel generators, where the equivalent sulphur mass fraction in the fuel must be as low as 0.1% in the

Table 6
Assumption and constraints for the ORC system optimization.

Parameter	Symbol	Value
Thermal oil pump isentropic efficiency	$\eta_{P,TO}$	60%
Working fluid pump isentropic efficiency	η_P	60%
Expansion machine isentropic efficiency	η_E	70%
Mechanical and electrical efficiencies of machines	η_m, η_e	100%
RECP effectiveness	η_{RECP}	80%
Exhaust gas specific heat capacity under constant pressure	$c_{p,EG}$	1.15 kJ/kg/K
Cooling water specific heat	$c_{p,cw}$	4.19 kJ/kg/K
Piping pressure losses in thermal oil, working fluid and coolingwater circuits	Δp_{pipes}	0 (not considered)
Thermal oil pressure losses in EGHX	$\Delta p_{TO,EGHX}$	80 mbar
Thermal oil pressure losses in TOHX	$\Delta p_{TO,TOHX}$	80 mbar
Working fluid pressure losses in TOHX, CWHX and RECP	$\Delta p_{wf,i}$	0 (not considered)
Cooling water pressure losses in CWHX	Δp_{cw}	0 (not considered)
Heat losses in piping and components	$\dot{Q}_{HL,i}$	0 (not considered)
Sub-cooling	ΔT_{subc}	2 °C
Condensation pressure	p_{cond}	1 bar
Cooling water inlet temperature	$T_{cw,in}$	25 °C
Exhaust gas temperature downstream EGHX	$T_{EG,EGHX,out}$	>85 °C
EGHX, TOHX, CWHX pinch temperature	$\Delta T_{pp,i}$	>10 °C
Evaporation pressure	p_{evap}	<min(0.9 × p_c, 30 bar)
Maximum working fluid temperature	$T_{wf,max}$	<T_c

Table 7
Independent variables for optimization procedure.

Thermal oil mass flow (kg/s)	$\dot{m}_{f,TO}$
Thermal oil EGHX inlet temperature [°C]	$T_{TO,in}$
Pump pressure ratio (–)	p_{ratio}
ORC working fluid mass flow (kg/s)	$\dot{m}_{f,wf}$
Superheating (°C)	ΔT_{suph}
Cooling water mass flow (kg/s)	$\dot{m}_{f,cw}$

Emission Control Areas (ECAs), an acid dew point temperature in the range of 85–90 °C can be expected.

3.4. ORC performance indexes

Together with the evaluation of the ORC net power output, which is used to compute the bsfc improvement of the combined engine-ORC configuration, various comprehensive ORC system performance indexes are also calculated, characterising the efficiency of the exploitation of the engine waste heat energy and the size and economics of the ORC system. Most of the indexes are obtained or re-elaborated from Branchini et al. [41], and are reported in Table 8.

In particular, the last index concerning heat transfer equipment dimensions, can be very useful, since the final decision regarding the selection of the most favorable cycle layout and organic working fluid, for the investigated turbocharging system scenarios and the relative engine configuration, should be ultimately based on a thermo-economic assessment, as reported by Quoilin et al. [42], followed by multi-criteria evaluation, as exemplified by Frangopoulos et al. [43], using technical, economic and environmental parameters.

The heat exchanger heat transfer coefficient UA_i is calculated using the Log Mean Temperature Difference method (LMTD) [44].

4. Results

In the following paragraphs the results of the thermodynamic process analysis and optimization of the engine and ORC systems are presented and discussed, with the purpose of finding the best configuration to increase the overall powertrain fuel efficiency.

4.1. Internal combustion engine and turbocharging

Fig. 5(a)–(l) shows various engine and turbocharging system parameters for the three investigated turbocharging systems, considering the effect of the increased backpressure due to the installation of the ORC boiler (ORC EGHX).

In order to facilitate the understanding of the results reported in the ORC section, the operating conditions for the considered simulated cases are extracted from Fig. 5(k)–(l) and reported in Table 9.

The case of the fixed turbocharging system can be used for the explanation of the main effects of the increasing backpressure. On the one hand, since the engine has to overcome higher pumping losses, while maintaining a constant brake load, more fuel has to be consumed resulting in the increase of the engine bsfc (positive Δbsfc, compared to reference base case engine bsfc). On the other hand, the turbine and, consequently compressor pressure ratios, are reduced, reducing accordingly the air mass flow through the engine. As a result, the trapped AFR is reduced, deteriorating the combustion quality. Moreover, the increased exhaust temperatures increase the thermal loading of the engine, which in turn can cause thermal failure of the pistons, cylinder heads and valves, as well as breakdown of the oil film, with adverse wear consequences on pistons and cylinder walls. However, the turbine inlet temperature never exceeds its allowable limit.

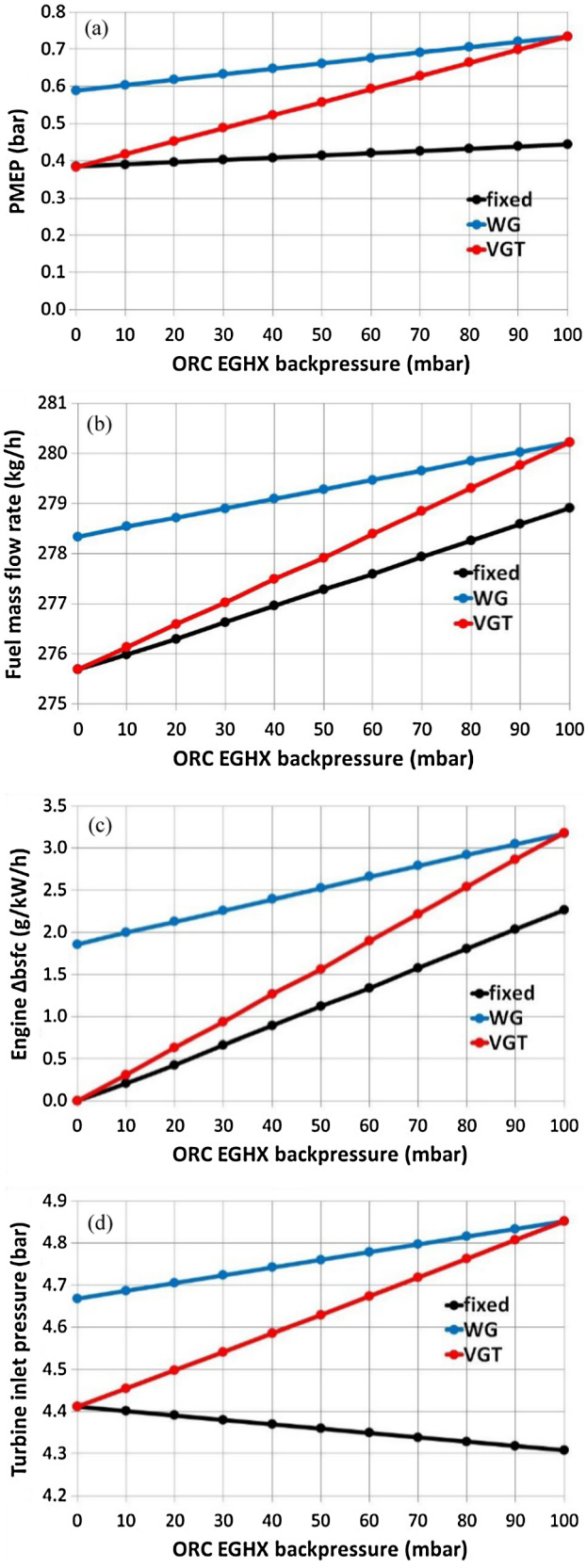

Fig. 5. PMEP (a), fuel mass flow rate (b), engine Δbsfc (c), turbine inlet pressure (d), turbine pressure ratio (e), compressor pressure ratio (f), air mass flow rate (g), AFR trapped (h), turbine inlet temperature (i), turbine outlet temperature (j), exhaust gas temperature upstream the EGHX (l), against ORC EGHX backpressure for the fixed, WG and VGT turbocharging system scenarios.

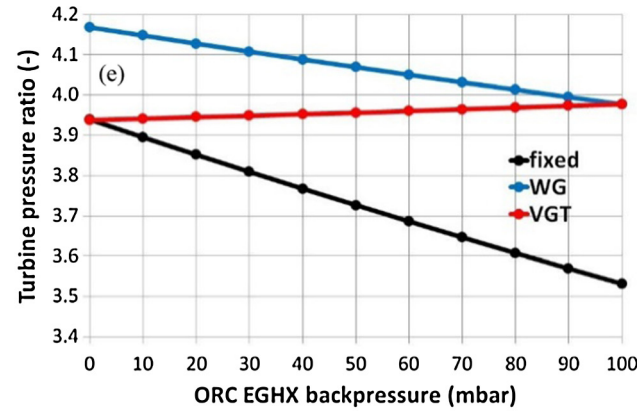

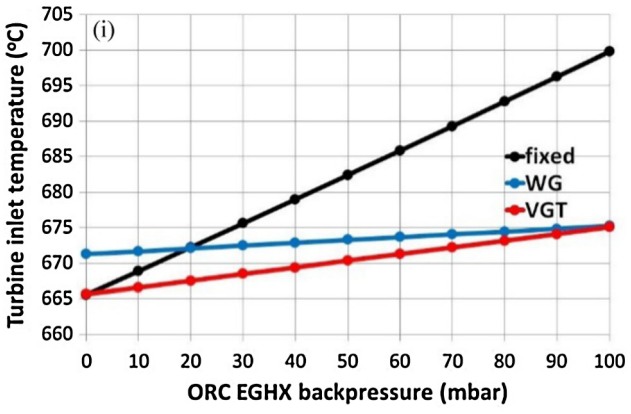

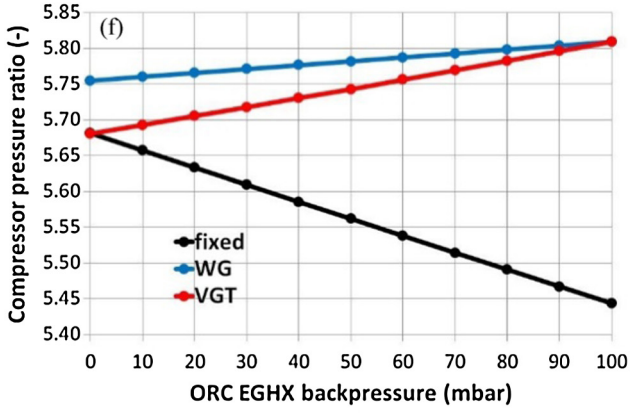

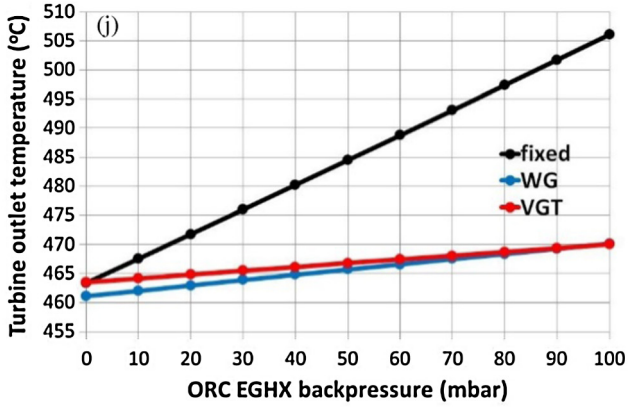

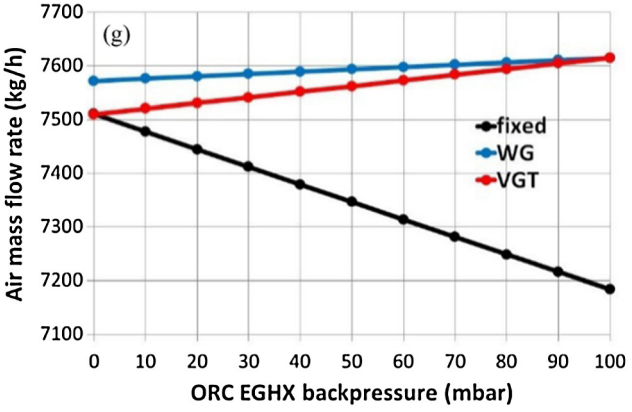

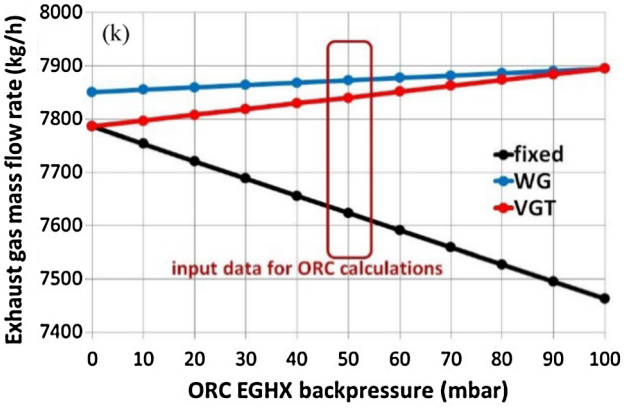

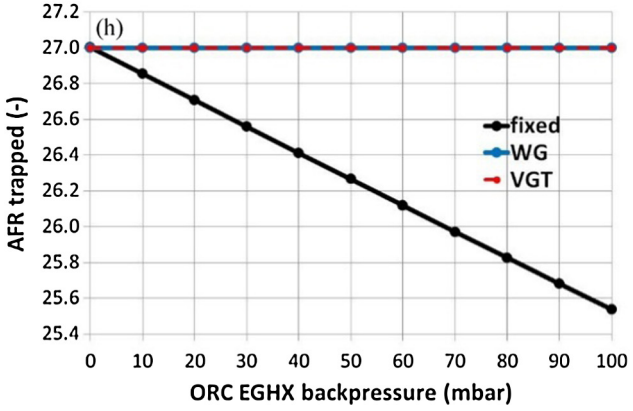

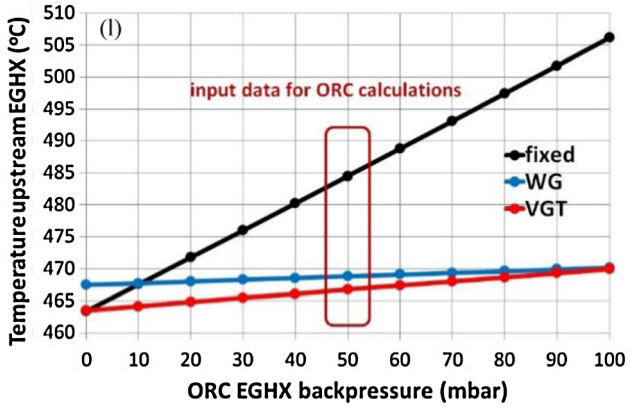

Fig. 5 (*continued*)

Fig. 5 (*continued*)

Table 8
ORC system performance indexes.

Index	Symbol	Significance	Aspect	Favorable trend
Thermal efficiency	$\eta_{ORC,th} = \frac{w_{ORC,net}}{q_{in}}$	Conversion efficiency of absorbed exhaust gas heat into useful power output	System efficiency	High
Specific work	$w_{ORC,net} = w_T - w_P$	Amount of organic fluid Required for an assigned power output	System efficiency	High
Organic fluid to exhaust gas mass flow ratio	$MFR = \frac{\dot{m}_{f,wf}}{\dot{m}_{f,EG}}$	amount of organic fluid required per unit of exhaust gas mass flow	System size	Low
Recovery efficiency	$\eta_{rec} = MFR \cdot \frac{w_{ORC,net}}{c_{p,EG} \cdot (T_{EG,in} - T_{EG,out,min})}$	Conversion efficiency of available exhaust gas heat into useful power output (proportional to the product of thermal efficiency and heat recovery process effectiveness)	System efficiency	High
Expander volumetric expansion ratio	$VER = \frac{v_{out}}{v_{in}}$	Expansion machine sizing (and possibly type) – ratio of specific fluid volumes over the expander	System size	Low
HXs surface index	$SI_{HX,ORC} = \frac{\sum_i UA_i}{\dot{m}_{f,EG}}$	Sum of HXs surface	System size	Low

Table 9
ORC boundary conditions for exhaust gas mass flow and temperature.

Parameter	Fixed geometry turbine	Waste-Gate (WG) turbine	Variable Geometry Turbine (VGT)
Exhaust gas mass flow, $\dot{m}_{f,EG}$ (kg/h)	7623.6	7872.6	7839.6
Exhaust gas temperature, $T_{EG,EGHX,in}$ (°C)	484.5	468.9	466.8

The first alternative to the fixed turbocharger, with the purpose of decreasing exhaust temperatures and maintaining the base case trapped AFR, is the use of a smaller turbine to increase the boost pressure, and therefore the engine air mass flow, equipped with a WG valve in order to bypass some of the exhaust gas around the turbine at the lower backpressure cases, when the requirements for increased boost pressure are reduced. The WG opening area is controlled so as to preserve, in all backpressure cases, the base case AFR. In comparison to the fixed turbocharger case, the pumping losses (PMEP, bar) are now increased, increasing fuel consumption in order to maintain the constant brake load, therefore resulting also in increased bsfc. As expected, the turbine pressure ratio is now increased, due to the smaller turbine size. As backpressure increases, the closing of the WG valve results in the increase of the pressure upstream the turbine. However, the turbine pressure ratio is continuously decreasing. Compressor pressure ratio is higher than that of the fixed turbocharger case, however this increases with backpressure, increasing respectively the air flow to such extent so as to keep the AFR fixed. Even though the bsfc of the engine is now higher, turbine inlet temperatures are in general lower than those of the fixed turbocharger case due to the higher AFRs, with this trend being reversed at the low backpressure cases, where the AFR of the fixed turbocharger case is still high and close enough to the base case value. Due to the higher turbine pressure ratio, turbine outlet temperatures are now reduced. However, finally due to the mixing with the hot bypass exhaust gas as backpressure reduces, the temperature upstream the EGHX is getting slightly higher at the low backpressure cases, however, with not very marked effect.

To reduce the increased bsfc due to the smaller turbine of the WG turbocharger case, while still maintaining the base case AFR, the solution of a VGT turbocharger is applied. The flexibility offered by the variable turbine nozzle area of the VGT turbocharger, being this practically correspondent to different turbine sizes for the various backpressure cases, results, on the one hand, in a turbine size equal to that of the fixed turbocharger at the 0 mbar backpressure case and, on the other hand, in a turbine size equal to that of the WG turbocharger at the 100 mbar backpressure case. In the intermediate backpressures, the turbine nozzle area of the VGT turbocharger is adjusted linearly between the two extreme cases. This trend for the VGT turbocharger, between the fixed and WG turbochargers at the 0 mbar and 100 mbar backpressure cases, respectively, can be obviously observed in the graphs of PMEP, fuel mass flow rate and engine Δbsfc. Therefore, in terms of engine efficiency, the VGT turbocharger offers a clear benefit over the WG for the investigated ORC backpressure effect. Additionally, it is observed that, as backpressure increases, the decrease of the turbine nozzle area throttles the exhaust gas flow to such an extent so that the turbine pressure ratio, even if slightly, increases continuously. Accordingly, the compressor pressure ratio and engine air mass flow are increased to maintain the base case AFR, following the above mentioned correlation between the fixed and WG turbochargers extreme backpressure cases. The turbine inlet temperature is reduced even further in comparison to the WG turbocharger case, following the relevant bsfc trends, since AFR is the same. However, the temperatures at the turbine exit appear to be higher than those of the WG turbocharger case due to the lower pressure ratio of the VGT turbocharger turbine. Finally, this trend reverses again, since, as already seen, the exhaust gas of the WG turbocharger is slightly heated again due to its mixing with the hot gas bypassing the WG turbocharger turbine.

From the engine operation point of view, it can be stated that, among the investigated turbocharging system scenarios, the VGT turbocharger seems to be the most favorable solution, alleviating at the most the adverse effect of the ORC EGHX backpressure on engine efficiency, while at the same time fulfilling the requirements for constant AFR and relatively low and safe exhaust temperatures.

In Fig. 5(k)–(l) and in Table 9, the boundary conditions, regarding temperatures and mass flow rates, for the ORC simulations are reported for the three considered turbocharging strategies.

4.2. ORC

In addition to the analysis of the backpressure effect on the engine side operations, it is useful to carry out a performance evaluation of the combined engine-ORC system, considering also the qualitative comparison of the trends of the ORC system performance indexes in the simulated cases. For this purpose, the results of the 1-D engine analysis, for a moderate EGHX backpressure of 50 mbar, are used as input for the ORC calculations, which consider a simple and a recuperated cycle layouts and *n*-hexane, *n*-octane, acetone, toluene, ethanol and MDM as working fluids. An optimization of the relevant cycle parameters with the purpose of maximizing the ORC net power output is carried out.

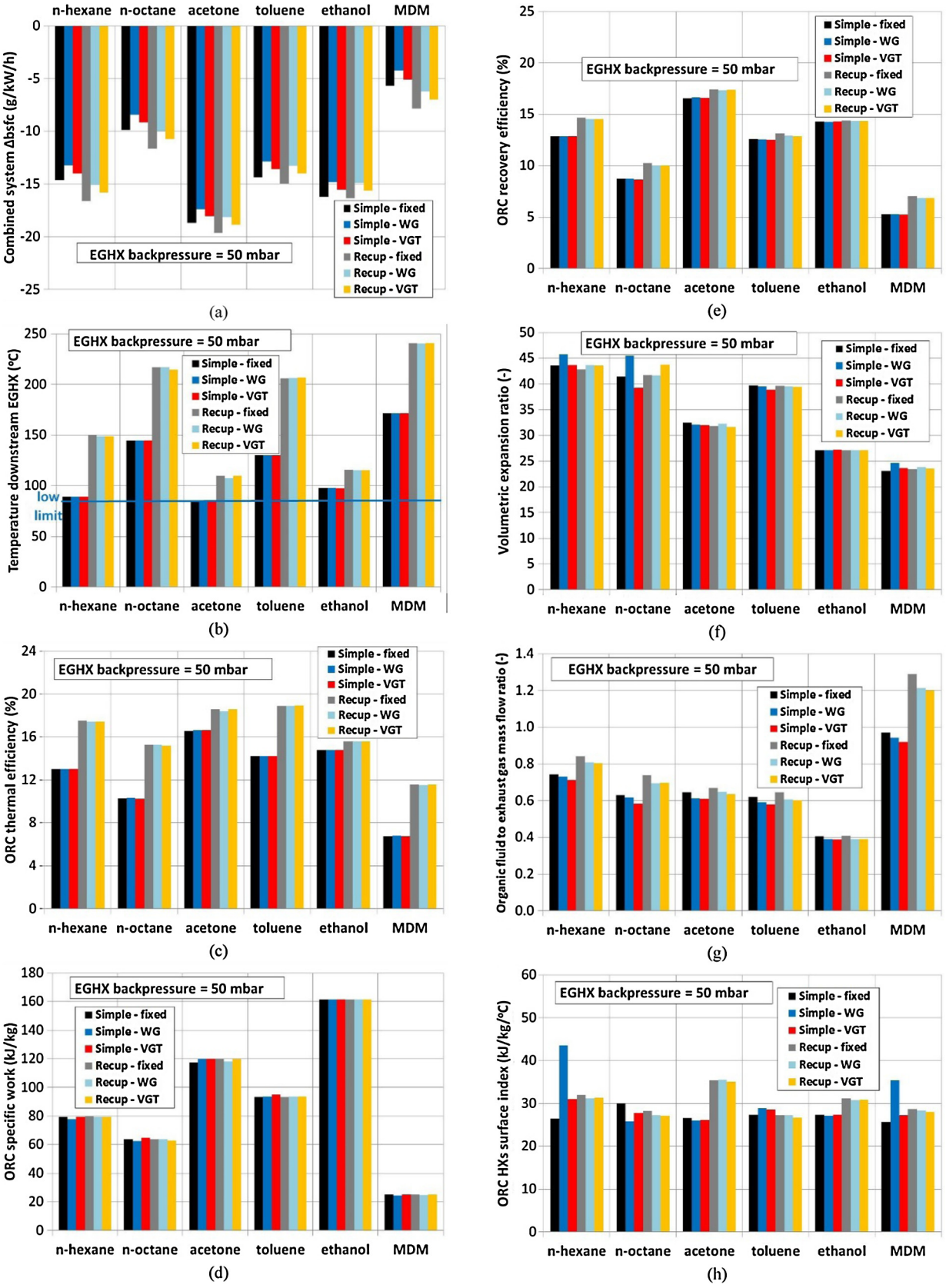

Fig. 6. Combined engine-ORC system Δbsfc (a), exhaust gas temperature downstream EGHX (b), ORC thermal efficiency (c), ORC specific work (d), ORC recovery efficiency (e), expansion machine volumetric expansion ratio (f), organic fluid to exhaust gas mass flow (g) and ORC HXs surface index (h) for the analysed working fluids and the simple and recuperated cycle layouts, with optimized cycle parameters and WG and VGT turbocharging scenarios.

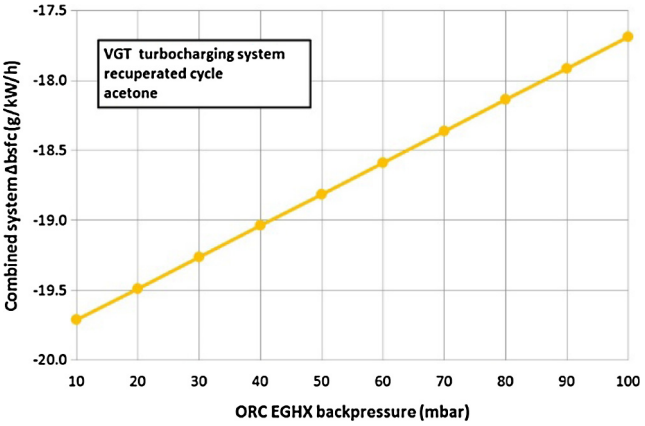

Fig. 7. Combined engine-ORC system Δbsfc against EGHX backpressure for the VGT turbocharging system with optimized recuperated ORC layout operated on acetone.

Fig. 6(a)–(h) shows the combined system Δbsfc reduction, the exhaust gas temperatures at the EGHX outlet, as well as the ORC system efficiency and size performance indexes for the investigated fluids and layouts combinations. As it can be observed, the main factor determining the combined system Δbsfc is the working fluid choice for the ORC system. In addition, as a general trend, it is observed that the recuperated cycle offers greater fuel economy, resulting at the same time in higher exhaust gas temperatures downstream the EGHX. Therefore, in this case, the exhaust gas can be further utilized. The VGT turbocharger, as well, provides always larger fuel economy benefits for the combined system than the WG turbocharger independently of cycle layout and working fluid, with the fixed turbocharger excluded from the comparison due to its inability to keep AFR constant, thus also influencing combustion efficiency and emissions patterns.

From the combined system efficiency point of view, it can be inferred that the largest fuel economy benefits are obtained with the recuperated cycle operating on acetone, with a VGT turbocharger on the engine side in order to keep the AFR constant, thus preserving a good combustion quality. According to the results, such a system shows the potential of reducing the bsfc approximately of 18.9 g/kWh (9.8% reduction), with the assumption of 50 mbar EGHX backpressure. This is mainly a result of the increased thermal and recovery efficiencies of this particular ORC system. As far as size and economics indexes are concerned, the recuperated acetone cycle presents relatively moderate requirements of expansion machine size and general system size (mass flow ratio index). However, its implementation involves relatively large, and therefore costly, heat exchangers.

After the identification of the most promising, in terms of combined system efficiency, turbocharging-ORC system configuration, based on the 50 mbar EGHX backpressure assumption, additional performance simulation runs of this system are conducted for the complete EGHX backpressure range, in order to evaluate the respective fuel economy benefit range that can be expected for any possible EGHX hardware design. According to Fig. 7, which presents the Δbsfc achieved by this particular combined system for the various EGHX backpressure values, it is shown that the effect of the EGHX design on the fuel consumption improvement is relatively weak, since the bsfc reduction that can be obtained lies between 17.7 and 19.7 g/kWh (9.1–10.2%).

5. Conclusions

This work investigates the possibility of introducing an ORC to improve the performance of a high speed diesel engine. In particular, the effects of introducing the ORC evaporator on the engine exhaust gas backpressure are considered.

Three turbocharging systems are considered: a fixed geometry turbocharger, a turbocharger with a Waste-Gate and a VGT turbocharger.

Some main considerations can be drawn:

- From the engine operation point of view, the VGT turbocharger is the most favorable solution, since it alleviates at the most the adverse effect of the ORC EGHX backpressure on engine efficiency while, at the same time, it fulfils the requirements for constant AFR and relatively low and safe exhaust temperatures.
- From the combined engine-ORC system efficiency point of view, the combination of the VGT turbocharger with a recuperated cycle operated with acetone provides the greatest benefits, reducing the bsfc of the combined system of 17.7–19.7 g/kWh (9.1–10.2%), depending on the EGHX backpressure. This is mainly due to the relatively high thermal and recovery efficiencies of this particular ORC configuration. In terms of size/economic issues, the selected ORC system presents relatively moderate requirements of expansion machine size and general system size in comparison to the other candidate solutions. However, its implementation requires the use of relatively large and costly heat transfer equipment.
- In general, the efficiency of the combined system depends mainly on the used organic working fluid, with the influence of the cycle layout and turbocharging system coming as subsequent requirements.
- In terms of cycle layouts, recuperated ORC configurations present clear efficiency benefits over their simple cycle counterparts, resulting also in favourably higher exhaust gas temperatures at their exhaust gas outlet for further use in typical cogeneration configurations.

In this work the internal combustion engine study has been carried out using fixed engine parameters. As a future work, engine parameters optimization will be carried out on the selected solution (VGT). Engine parameters to be considered are, for example, the valve timing, valve diameters, injection timing and compression ratio.

For the final selection of the most favorable cycle layout and working fluid, a thermo-economic assessment, followed by a multi-criteria evaluation of the investigated ORC systems, could integrate the thermodynamic results of this work. For this reason, the technical parameters computed could be used as input into cost functions of the ORC components to evaluate relevant economic parameters. Subsequently, technical, economic and environmental parameters could be introduced using an appropriate multi-criteria evaluation procedure in order to obtain an index to be used for the final quantitative comparison of the various examined system configurations.

Acknowledgments

The research leading to these results has received funding from the People Programme (Marie Curie Actions) of the European Union's Seventh Framework Programme FP7/2007-2013/ under REA grant agreement no. 607214.

References

[1] Marindagen S, Haraldson L. Potentialer för verkningsgradsförbättringar – EffShip Project. Wärtsilä; 2011.
[2] OPCON Marine – OES OPCON Technology; n.d. <http://opconenergysystem.com/en/opcon-marine-3/> [accessed April 24, 2016].
[3] Turboden and Wärtsilä sign agreement to launch Wärtsilä Marine ECC. Turboden, press release; 2010.

[4] Yuksek EL, Mirmobin P. Waste heat utilization of main propulsion engine jacket water in marine application. In: ASME ORC 2015 proc 3rd int semin ORC power syst.
[5] Swain E. Turbocharging the submarine diesel engine. Mechatronics 1994;4:349–67.
[6] Swain E, Elliot C. Controlling a variable-geometry turbine nozzle on a turbocharger fitted to a diesel engine in a submarine environment. Inst Mech Eng 1994;6:175–85.
[7] Smith TM, Newman JM. A variable geometry turbocharger for a submarine diesel engine. Inst Mech Eng 1994;6:187–201.
[8] Herrmann R. Combined supercharging system: the best fit for submarines. In: 2001 spring tech conf ASME intern combust engine div ASME.
[9] Hield P. The effect of back pressure on the operation of a diesel engine. Technical report. Australian Government. Department of Defence; 2011.
[10] Katsanos C, Hountalas DT, Pariotis EG. Thermodynamic analysis of a Rankine cycle applied on a diesel truck engine using steam and organic medium. Energy Convers Manage 2012;60:68–76. http://dx.doi.org/10.1016/j.enconman.2011.12.026.
[11] Horst TA, Tegethoff W, Eilts P, Koehler J. Prediction of dynamic Rankine Cycle waste heat recovery performance and fuel saving potential in passenger car applications considering interactions with vehicles' energy management. Energy Convers Manage 2014;78:438–51. http://dx.doi.org/10.1016/j.enconman.2013.10.074.
[12] Bei C, Zhang H, Yang F, Song S, Wang E, Liu H, et al. Performance analysis of an evaporator for a diesel Engine-Organic Rankine Cycle (ORC) combined system and influence of pressure drop on the diesel engine operating characteristics. Energies 2015;8:5488–515. http://dx.doi.org/10.3390/en8065488.
[13] Di Battista D, Mauriello M, Cipollone R. Waste heat recovery of an ORC-based power unit in a turbocharged diesel engine propelling a light duty vehicle. Appl Energy 2015;152:109–20. http://dx.doi.org/10.1016/j.apenergy.2015.04.088.
[14] Allouache A, Leggett S, Hall MJ, Tu M, Baker C, Fateh H. Simulation of organic rankine cycle power generation with exhaust heat recovery from a 15 L diesel engine. SAE Int J Mater Manuf 2015;8. http://dx.doi.org/10.4271/2015-01-0339.
[15] Yamaguchi T, Aoyagi Y, Uchida N, Fukunaga A, Kobayashi M, Adachi T, et al. Fundamental study of waste heat recovery in the high boosted 6-cylinder heavy duty diesel engine. SAE Int J Mater Manuf 2015;8. http://dx.doi.org/10.4271/2015-01-032.
[16] Song J, Yin S, Gu C. Thermodynamic analysis and performance optimization of an ORC (Organic Rankine Cycle) waste heat recovery system for marine diesel engines. Energy 2015;82:976–85. http://dx.doi.org/10.1016/j.energy.2014.05.014.
[17] Reini M, Pinamonti P. Different options for ORC's as bottom for an internal combustion engine for ship propulsion. Energies 2015.
[18] Burel F, Taccani R, Zuliani N. Improving sustainability of maritime transport through utilization of Liquefied Natural Gas (LNG) for propulsion. Energy 2013;57:412–20. http://dx.doi.org/10.1016/j.energy.2013.05.002.
[19] Baldi F, Gabrielii C. A feasibility analysis of waste heat recovery systems for marine applications. Energy 2015.
[20] Baldi F, Larsen U, Gabrielii C. Comparison of different procedures for the optimisation of a combined diesel engine and organic Rankine cycle system based on ship operational profile. Ocean Eng 2015;110:85–93. http://dx.doi.org/10.1016/j.oceaneng.2015.09.037.
[21] Yun E, Park H, Yoon SY, Kim KC. Dual parallel organic Rankine cycle (ORC) system for high efficiency waste heat recovery in marine application. J Mech Sci Technol 2015;29:2509–15. http://dx.doi.org/10.1007/s12206-015-0548-5.
[22] Yfantis EA, Katsanis IS, Pariotis EG, Zannis TC, Papagiannakis RG. First-law and second-law waste heat recovery analysis of a four-stroke marine diesel engine equipped with a regenerative organic rankine cycle system. In: 5th Int symp sh oper manage. p. 1–11.
[23] Hountalas DT, Katsanos C, Mavropoulos GC. Efficiency improvement of large scale 2-stroke diesel engines through the recovery of exhaust gas using a Rankine cycle. Procedia – Soc Behav Sci 2012;48:1444–53. http://dx.doi.org/10.1016/j.sbspro.2012.06.1120.
[24] Larsen U, Pierobon L, Haglind F, Gabrielii C. Design and optimisation of organic Rankine cycles for waste heat recovery in marine applications using the principles of natural selection. Energy 2013;55:803–12. http://dx.doi.org/10.1016/j.energy.2013.03.021.
[25] Yang M-H. Thermal and economic analyses of a compact waste heat recovering system for the marine diesel engine using transcritical Rankine cycle. Energy Convers Manage 2015;106:1082–96. http://dx.doi.org/10.1016/j.enconman.2015.10.050.
[26] Yang M-H, Yeh R-H. Analyzing the optimization of an organic Rankine cycle system for recovering waste heat from a large marine engine containing a cooling water system. Energy Convers Manage 2014;88:999–1010. http://dx.doi.org/10.1016/j.enconman.2014.09.044.
[27] Ricardo Software. Ricardo WAVE; n.d. <http://www.ricardo.com/en-GB/What-we-do/Software/Products/WAVE/> [accessed February 4, 2016].
[28] F-Chart Software. Engineering Equation Solver (EES); n.d. <http://www.fchart.com/ees/> [accessed February 5, 2016].
[29] Ricardo. EMLEG – Emissions Legislation Database; n.d. <http://www.emleg.com/> [accessed September 1, 2015].
[30] Qiu T, Li X, Liang H, Liu X, Lei Y. A method for estimating the temperature downstream of the SCR (selective catalytic reduction) catalyst in diesel engines. Energy 2014;68:311–7. http://dx.doi.org/10.1016/j.energy.2014.02.101.
[31] Woodyard D. Pounders – marine diesel engines and gas turbines, 9th ed., 2009.
[32] Heim K. Existing and future demands on the turbocharging of modern large two-stroke diesel engines. In: 8-th Supercharging conf Dresden. p. 1–18.
[33] Saidur R, Rezaei M, Muzammil WK, Hassan MH, Paria S, Hasanuzzaman M. Technologies to recover exhaust heat from internal combustion engines. Renew Sustain Energy Rev 2012;16:5649–59. http://dx.doi.org/10.1016/j.rser.2012.05.018.
[34] Downtherm Q. Heat transfer fluid. Product technical data. The Dow Chemical Company; n.d.
[35] The montreal protocol on substances that deplete the ozone layer – UNEP, Ozone secretariat united nations environment programme; 2000.
[36] Kyoto protocol to the United Nations framework convention on climate change. United Nations; 1998.
[37] Saleh B, Koglbauer G, Wendland M, Fischer J. Working fluids for low-temperature organic Rankine cycles. Energy 2007;32:1210–21. http://dx.doi.org/10.1016/j.energy.2006.07.001.
[38] Lai NA, Wendland M, Fischer J. Working fluids for high-temperature organic Rankine cycles. Energy 2011;36:199–211. http://dx.doi.org/10.1016/j.energy.2010.10.051.
[39] NFPA 704: Standard system for the identification of the hazards of materials for emergency response, 2017 ed. National Fire Protection Association; 2017.
[40] Lemmon EW, Huber ML, McLinden MO. NIST standard reference database 23: reference fluid thermodynamic and transport properties-REFPROP 2013; n.d.
[41] Branchini L, De Pascale A, Peretto A. Systematic comparison of ORC configurations by means of comprehensive performance indexes. Appl Therm Eng 2013;61:129–40. http://dx.doi.org/10.1016/j.applthermaleng.2013.07.039.
[42] Quoilin S, Declaye S, Tchanche BF, Lemort V. Thermo-economic optimization of waste heat recovery Organic Rankine Cycles. Appl Therm Eng 2011;31:2885–93. http://dx.doi.org/10.1016/j.applthermaleng.2011.05.014.
[43] Frangopoulos CA, Keramioti DE. Multi-criteria evaluation of energy systems with sustainability considerations. Entropy 2010;12:1006–20. http://dx.doi.org/10.3390/e12051006.
[44] Incropera FP, DeWitt DP, Bergman TL, Lavine A. Fundamentals of heat and mass transfer. 6th ed. Wiley; 2007.